Journal of Applied Sciences

ISSN 1812-5654

Journal of Applied Sciences 10 (4): 354-358, 2010
ISSN 1812-5654

Effects of Gaussian Filtering on Processing Gain in Acousto-Optic Correlators

O. Bazzi, A. Alaeddine, Y. Mohanna and A. Hafiz
Department of Physics and Electronics, Faculty of Sciences1,
Lebanese University, Hadath, Beirut, Lebanon

Abstract: The effects of Gaussian filtering on the processing gain of Acousto-Optic Correlators (AOC) in direct-sequence spread-spectrum receivers are considered. Analytical expressions are derived for ideal AOC's. The results are given in terms of the ratio β of the code chip rate to the filter bandwidth. For real AOC's, results are obtained from numerical simulation and are compared to previous results obtained for other types of filters.

Key words: Acousto-optics, correlation, Gaussian filtering, signal to noise ratio

INTRODUCTION

Acousto-optic devices are still considered attractive for processing signal and images as they offer real-time operation and high dynamic range (Berg and Lee, 1991; Balakshy and Kostyuk, 2009; Korpel, 2009). Acousto-Optic Correlators (AOC) used with Spread-Spectrum (SS) signals figure among the valuable applications. Different architectures of AOC are described in literature (Bazzi *et al*., 1994; Kim *et al*., 2004; Gurevich *et al*., 2004). The effects of integrating the AOC in a spread-spectrum receiver are reported by Bazzi *et al*. (2006) where the receiver equivalent model in the baseband is reduced to a low-pass filter acting on the received signal. The results show a processing gain reduction which is filter dependent.

The effects of Gaussian filtering in the receiver are presented in this study. Gaussian filtering is particularly effective when used in conjunction with Minimum Shift Keying (MSK) modulation or other modulations which are suited for power-efficient nonlinear amplifiers (Rappaport, 2002). The receiver model is first briefly reviewed. Analytical results are then derived for ideal AOC. For real AOC's, results are obtained from numerical simulation and are compared to previous results obtained for two other types of filters: ideal low-pass and RC filters.

THE SS RECEIVER MODEL

Figure 1 shows a view of the equivalent SS receiver diagram using an AOC. The received SS signal is down-converted into baseband before performing correlation with a reference code. We distinguish the two filters of frequency responses $H_1(f)$ and $H_2(f)$ where:

Filter $H_1(f)$ is proper to the AOC. It represents the acousto-optic interaction frequency response and affects both the received and the reference signals. The equivalent normalized baseband representation of $H_1(f)$ is (Bazzi *et al*., 1996):

$$H_1(f) = \text{sinc}\left(\frac{f}{\Delta f}\right) \quad (1)$$

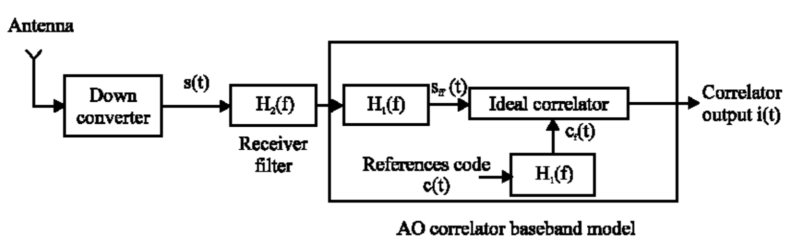

Fig. 1: Equivalent diagram for the SS receiver with an embedded AOC

Corresponding Author: Oussama Bazzi, Department of Physics and Electronics, Faculty of Sciences1, Lebanese University, Hadath, Beirut, Lebanon Tel: 00 961 5 460494 Fax: 00 961 5 461496

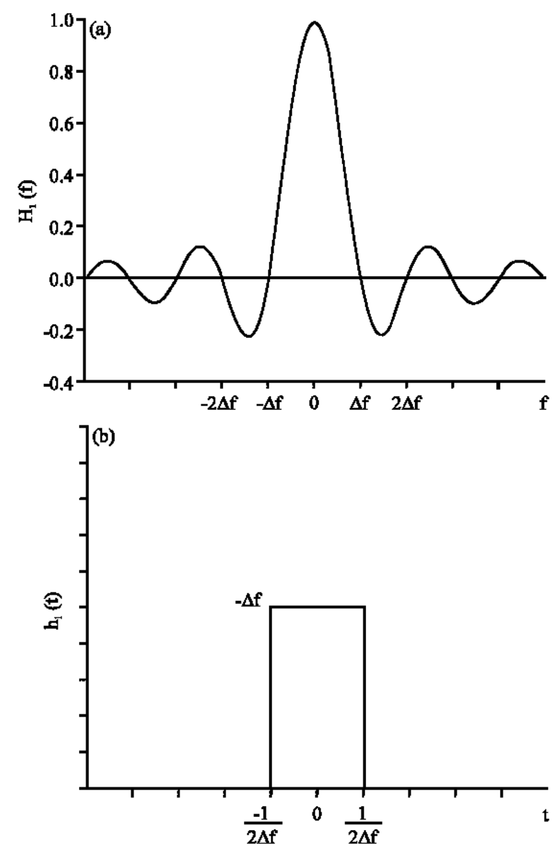

Fig. 2: AO normalized correlator response: (a) Frequency response and (b) impulse response

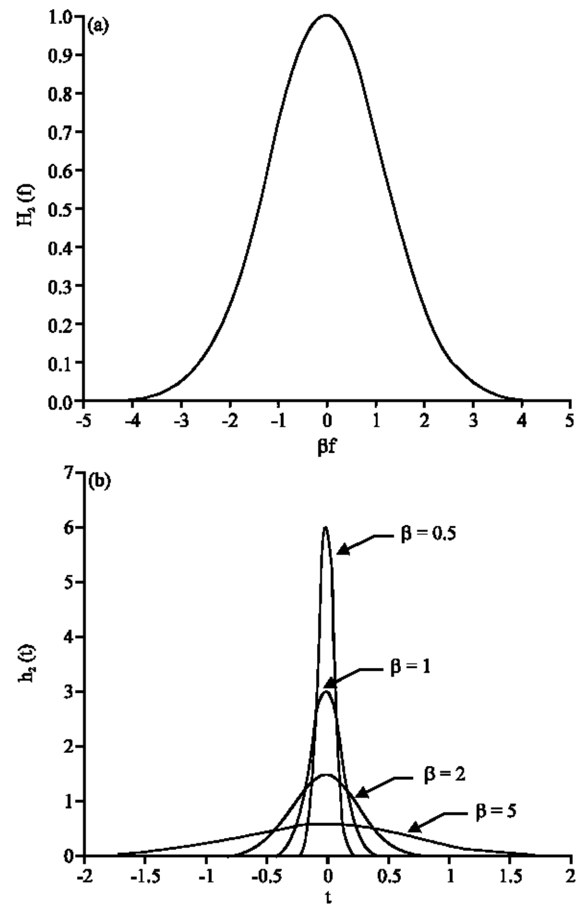

Fig. 3: Gaussian filter response: (a) Frequency response and (b) impulse response

where,

$$\text{sinc}\ (x) = \frac{\sin(\pi x)}{\pi x}$$

f is the acoustic frequency and Δf is the cutoff frequency at -4dB corresponding to half the first-null bandwidth. The normalized response of the AOC is presented in Fig. 2a and b.

Filter $H_2(f)$ is the receiver filter which characterizes the receiver channel. This filter affects the received signal. The baseband Gaussian characteristics, considered in this study, is given by:

$$H_2(f) = \exp(-a^2 f^2) \tag{2}$$

where, the parameter a is related to the 3 dB bandwidth B of the Gaussian shaping filter by Rappaport (2002) :

$$a = \frac{\sqrt{\ln 2}}{\sqrt{2}B} = \frac{0.5887}{B} = 0.5887\ \beta \tag{3}$$

where, β is the inverse of the filter bandwidth.

Figure 3a and b show the frequency response $H_2(f)$ and the time response $h_2(t)$ of the Gaussian filter.

ANALYSIS OF THE RECEIVER PERFORMANCE

The analysis is done under the conventional pseudo-random sequence correlation where the received signal is correlated in the receiver with a locally generated reference code c(t) as shown in Fig. 1. The received signal s(t) consists of a desired signal Ac(t) corrupted by an additive zero-mean white Gaussian noise of Power Spectral Density (PSD) equal to η:

$$s(t) = Ac(t)+n(t) \tag{4}$$

where, A is the amplitude of the received signal, n(t) denotes a sample function of the noise process.

At the receiver input the signal to noise ratio is defined as (Proakis, 2000):

Table 1: Code characteristics

Single-chip : $\varepsilon(t) = rect(t)$	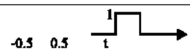
Autocorrelation : $C_{cc}(t) = tri(t)$	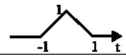

$$(SNR)_i = \frac{A^2}{\sigma_i^2} = \frac{A^2}{\eta} \quad (5)$$

where, σ_i^2 is the input noise power computed in a bandwidth equal to the chip rate which is, for convenience, normalized to one.

The processing gain is defined as the enhancement obtained in the Signal to Noise Ratio (SNR) as the signal goes through the receiver. In an ideal receiver (infinite bandwidth), the processing gain is equal to the spreading factor N i.e., the number of chips in the code period (Dixon, 1976). When N is large, the autocorrelation of the code can be approximated by Dixon (1976):

$$C_{cc}(t) = tri(t) \quad (6)$$

where, the chip rate is normalized to one and tri(t) = 1-abs(t) for abs(t)<1 and 0 otherwise. Table 1 shows the autocorrelation characteristics of the code chip $\varepsilon(t)$.

At the receiver output, referring to Fig. 1, the signal obtained is:

$$i(t) = \frac{1}{N}[S_{ff}(t) * c_f^N(-t)] \quad (7)$$

where, * is the convolution operator, the reference code is time-reversed in order to obtain correlation. The subscript (ff) refers to a two-stage filtering of signals: first in the receiver filter and second in the AO correlator. The subscript (f) refers to AO filtering alone. The superscript N refers to a single period of the code given by:

$$c^N(t) = c(t)rect(\frac{t}{N}) \quad (8)$$

where, rect(x) = 1 for abs(x)<0.5 and 0 otherwise:

Eq. 7 can be split as:

$$\begin{aligned} i(t) &= \frac{1}{N}[A_{cff}(t) + n_{ff}(t)] * c_f^N(-t) \\ &= \frac{A}{N}[c_{ff}(t) * c_f^N(-t)] + \frac{1}{N}[n_{ff}(t) * c_f^N(-t)] \\ &= s_0(t) + n_0(t) \end{aligned} \quad (9)$$

where, $s_0(t)$ and $n_0(t)$ represent, respectively signal and noise at the correlator output.

The Signal to Noise Ratio $(SNR)_0$ at the correlator output is defined as the ratio of the signal correlation peak power $\overline{s_0(0)}^2$, at the coincidence instant, to the output noise variance σ_0^2 (Proakis, 2000):

$$(SNR)_0 = \frac{\overline{s_0(0)}^2}{\sigma_0^2} \quad (10)$$

Using Eq. 5 and 10, the SNRE can be written as:

$$SNRE = \frac{(SNR)_0}{(SNR)_i} = \frac{\eta}{A^2\sigma_0^2}\overline{s_0(0)}^2 \quad (11)$$

Signal and noise analysis: The detailed analysis of $s_0(t)$ and $n_0(t)$ is found by Bazzi *et al*. (2006). The expressions for $s_0(t)$ and $C_{n0n0}(t)$ are given by:

$$s_0(t) = A\,[C_{cc}(t) * C_{h1h1}(t) * h_2(t)] \quad (12)$$

and

$$C_{n0n0}(t) = \frac{1}{N}\eta C_{h1h1}(t) * C_{h1h1}(t) * C_{cc}(t) * C_{h2h2}(t) \quad (13)$$

where, $h_1(t)$ and $h_2(t)$ are the impulse responses of the AO correlator and the receiver filter, respectively. $C_{xx}(t)$ denotes the autocorrelation of x(t).

The output noise variance is given by the autocorrelation peak value $C_{n0n0}(0)$ in Eq. 13.

Analysis of the correlator performance: The performance is studied in terms of two parameters:

- The ratio β of the code chip rate (normalized to one) to the cutoff frequency Δf of the AOC:

$$\alpha = \frac{1}{\Delta f} \quad (14)$$

- The ratio β of the code chip rate to the receiver filter bandwidth

α and β represent the filtering acuteness of the AOC and the receiver filter, respectively. Table 2 shows the impulse response characteristics of the AO correlator and the Gaussian filter used in the receiver.

ANALYTICAL RESULTS

Analytical results of the SNRE in the system are found in the case of ideal AOC ($H_1(f)=1$).

Eq. 12 and 13 reduce, in this case, to:

$$s_0(t) = AC_{cc}(t) * h_2(t) \quad (15)$$

Table 2: AO correlator and Gaussian receiver filter characteristics

System	Frequency response	Impulse response	Impulse-response autocorrelation
AO correlator	$H_1(f) = \text{sinc}\ (\alpha f)\ (\alpha = \frac{1}{\Delta f})$	$h_1(t) = \frac{1}{\alpha}\ \text{rect}\ (\frac{t}{\alpha})$	$C_{h1h1}(t) = \frac{1}{\alpha}\ \text{tri}(\frac{t}{\alpha})$
Gaussian filter	$H_2(f) = \exp(-a^2f^2)\ (a = 0.5887\beta)$	$h_2(t) = \frac{\sqrt{\pi}}{a}\exp(\frac{-\pi^2t^2}{a^2})$	$C_{h2h2}\ (t) = \frac{\sqrt{\pi}}{a\sqrt{2}}\exp(\frac{-\pi^2t^2}{2a^2})$

and

$$C_{r0r0}\ (t) = \eta/N\ [\ C_{cc}\ (t)^*\ C_{h2h2}\ (t)] \tag{16}$$

The autocorrelation function $C_{h2h2}(t)$ for the Gaussian filter is found in Table 2. The correlator output signal is given from Eq. 15 as:

$$s_0(t) = A\text{tri}(t)^*\frac{\sqrt{\pi}}{a}\exp(\frac{-\pi^2t^2}{a^2}) \tag{17}$$

The maximal signal value $s_0(0)$ is given by:

$$\begin{aligned} s_0(0) &= \frac{A\sqrt{\pi}}{a}\left[\int_{-1}^{0}(1+\lambda)e^{\frac{-\pi^2\lambda^2}{a^2}}d\lambda + \int_{0}^{1}(1-\lambda)e^{\frac{-\pi^2\lambda^2}{a^2}}d\lambda\right] \\ &= \frac{2A\sqrt{\pi}}{a}\left[\int_{0}^{1}e^{\frac{-\pi^2\lambda^2}{a^2}}d\lambda - \int_{0}^{1}\lambda e^{\frac{-\pi^2\lambda^2}{a^2}}d\lambda\right] \\ &= A[1-2\text{Erfc}(\frac{\sqrt{2}\pi}{a})]\text{-}\frac{Aa}{\pi\sqrt{\pi}}(1-e^{-\frac{\pi^2}{a^2}}) \end{aligned} \tag{18}$$

where, Erfc(x) is the Complementary Error function defined as:

$$\text{Erfc}(x) = \int_{x}^{\infty}\frac{1}{\sqrt{2\pi}}e^{\frac{-\lambda^2}{2}}d\lambda \tag{19}$$

Similarly, the noise variance at the correlator output is computed as:

$$\begin{aligned} \sigma_0^2 = C_{n0n0}(0) &= \frac{\eta}{N}\left[\text{tri}(t)^*\frac{\sqrt{\pi}}{a\sqrt{2}}\exp(\frac{-\pi^2t^2}{2a^2})\right]_{(t=0)} \\ &= \frac{\eta}{N}\frac{\sqrt{\pi/2}}{a}\left[\int_{-1}^{0}(1+\lambda)e^{\frac{-\pi^2\lambda^2}{2a^2}}d\lambda + \int_{0}^{1}(1-\lambda)e^{\frac{-p^2\lambda^2}{2a^2}}d\lambda\right] \\ &= \frac{\eta}{N}\ [1\text{-}2\text{Erfc}(\frac{\pi}{a}) - \frac{a\sqrt{2\pi}}{\pi^2}(1-e^{\frac{-\pi^2}{2a^2}})] \end{aligned} \tag{20}$$

The SNRE enhancement ratio is obtained, in terms of β, by replacing Eq. 18 and 20 in Eq. 11.

The SNRE loss compared to the ideal system is presented in Fig. 4 along with the signal and noise power reductions at the correlator output. In Fig. 5, the Gaussian filter effect is compared to the effects obtained previously for RC and ideal low-pass receiver filters (Bazzi *et al*., 2006). The figure shows that for β<2.5 the Gaussian filter and the RC filter have almost the same performance. For β = 5, an approximate SNRE loss of 1.8 dB is obtained with the Gaussian filter as compared to respective losses of 1.2 and 4.2 dB for RC and ideal low-pass filters.

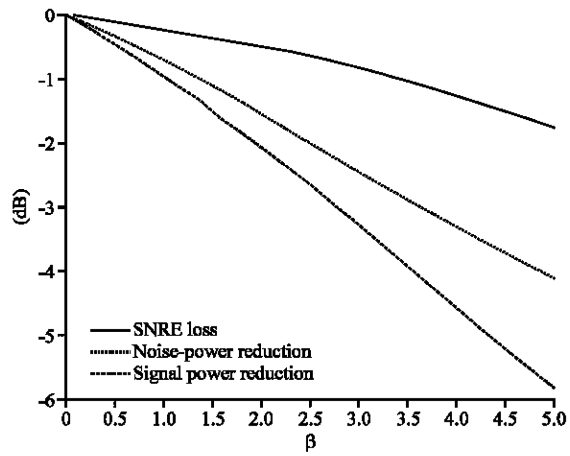

Fig. 4: Effects of the receiver Gaussian filter (ideal AOC)

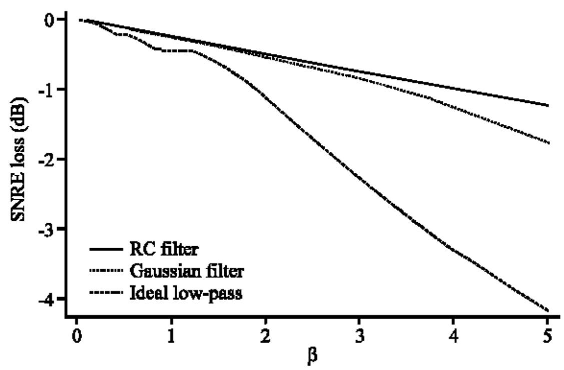

Fig. 5: SNRE losses for different receiver filters (ideal AOC)

NUMERICAL RESULTS

Results in the general case of a real AOC are obtained from numerical simulation of the system (receiver + correlator) as defined in Fig. 1.

The value N has been taken equal to 1023 with 100 samples per chip.

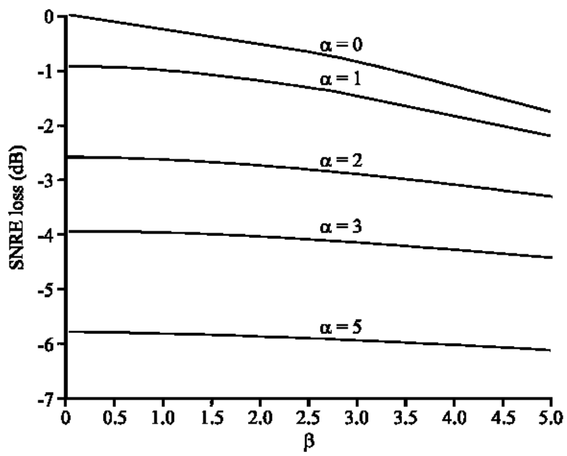

Fig. 6: SNRE loss in real AOC with Gaussian receiver filter

Results are presented in Fig. 6 in terms of the Gaussian filter parameter β for different values of the AOC acuteness factor α. For α = 0 (ideal AOC), the simulation results agree well with the analytical results.

We also see that as α increases the curves become broader and the AOC filtering effects become dominant.

CONCLUSION

Analysis of the effects of signal filtering on Acousto-Optic correlator performance is extended to the case of Gaussian filtering commonly used with MSK modulation. Analytical results were derived for ideal AOC in terms of the ratio β of the chip rate to the filter bandwidth. Numerical results were found in the general case. The detailed performance obtained will help optimize an equalizer for this kind of filter in order to reduce the processing gain loss in the correlator.

ACKNOWLEDGMENT

This work was supported by the National Council for Scientific Research - Lebanon.

REFERENCES

Balakshy, V.I. and D.E. Kostyuk, 2009. Acousto-optic image processing. Applied Optics, 48: C24-C32.

Bazzi, O., R.J. Torguet, C. Bruneel, M.G. Gazalet and J.M. Rouvaen, 1994. Space-integrating acousto-optic processor for rapid global positioning system signal acquisition. Optic Eng., 33: 2931-2935.

Bazzi, O., M.G. Gazalet, R.J. Torguet, J. M. Rouvaen and C. Bruneel, 1996. Effects of acousto-optic correlator bandwidth on coded pulse compression. Optic Eng., 35: 1656-1661.

Bazzi, O., M.G. Gazalet, Y. Mohanna, A. Alaeddine and A. Hafiz, 2006. Study of the effects of signal filtering on acousto-optic correlator performance. Optic Eng., 45: 1-7.

Berg, N.J. and J.N. Lee, 1991. Acousto-Optic Signal Processing. 1st Edn., Artech House Publisher, New York, ISBN: 0824716671.

Dixon, R.C., 1976. Spread Spectrum Systems with Commercial Applications. 3rd Edn., John Wiley and Sons, New York, ISBN: 9780471593423.

Gurevich, B., S. Andreyev, A. Belyaev, C. Akimjanova and K. Sagymbaeva, 2004. RF signal analysis using combined acousto-optical correlator and spectrum analyzer. Proc. SPIE, 5477: 330-334.

Kim, S., R. Narayanan, W. Zhou and K. Wagner, 2004. Time-integrating acousto-optic correlator for wideband random noise radar. Proc. SPIE, 5557: 216-222.

Korpel, A., 2009. The serendipity of acousto-optics. Applied Optics, 48: C1-C3.

Proakis, G.J., 2000. Digital Communications. 4th Edn., MacGraw-Hill, New York, ISBN: 0072321113.

Rappaport, T.S., 2002. Wireless Communications: Principles and Practice. 2nd Edn., Prentice Hall, UK., ISBN: 0130422320.